Journal of Solid Mechanics Vol. 3, No. 1 (2011) pp. 96-113

Nonlinear Finite Element Analysis of Bending of Straight Beams Using *hp*-Spectral Approximations

R. Ranjan*

SiViRT Center, University of Texas, San Antonio Department of Mechanical Engineering San Antonio, TX 78240

Received 4 January 2011; accepted 30 April 2011

ABSTRACT

Displacement finite element models of various beam theories have been developed using traditional finite element interpolations (i.e., Hermite cubic or equi-spaced Lagrange functions). Various finite element models of beams differ from each other in the choice of the interpolation functions used for the transverse deflection w, total rotation φ and/or shear strain γ_{xz}, or in the integral form used (e.g., weak form or least-squares) to develop the finite element model. The present study is concerned with the development of alternative beam finite elements using *hp*-spectral nodal expansions to eliminate shear and membrane locking. Both linear and non-linear analysis are carried out using both displacement and mixed finite element models of the beam theories studied. Results obtained are compared with both analytical (series) solutions and non-linear finite element solutions from literature, and excellent agreement is found for all cases.

Keywords: spectral/hp method; Timoshenko beam theory; Euler-Bernoulli Beam Theory; Nodal expansions; Displacement and mixed finite element models.

1 INTRODUCTION

THREE different kinematic theories have been used to study beams, namely, the Euler-Bernoulli theory (EBT), the Timoshenko beam theory (TBT), and Reddy third-order shear deformation theory (RBT). The displacement finite element models of TBT and RBT are known to exhibit shear locking when using equal-order, lower-order interpolation of the generalized displacements (w, φ). Locking is due to inconsistency of the interpolation used for w and φ. Often reduced-order integration techniques are used to alleviate locking [1]. The reduced integration beam elements are known to exhibit spurious energy modes. Others have used so-called consistent interpolation based on the recovery of correct constraints in the thick beam limit [2, 3]. Although such elements do not experience locking, they did not lead to the two-node super-convergent element developed by Reddy et al. [4], who used the Hermite cubic interpolation of w and *interdependent* quadratic interpolation of φ in developing the element. The conventional reduced integration Timoshenko elements as well as consistent interpolated quadratic elements fail to capture the true behavior of such members unless two or more elements per structural member are used.

While the displacement-based models for the Timoshenko beam theory (TBT) admit the use of C^0 expansions, the use of Euler Bernoulli beam theory (EBT) requires the use of C^1-continuous expansions. The mixed formulation in which stress resultants are incorporated into the fundamental governing equations for the Euler-Bernoulli beam theory admits the use of C^0 expansions, which naturally lends itself to spectral accuracy with the help of spectral expansions and reduced continuity requirements. The TBT, on the other hand, allows the use of C^0 approximations for the displacement based formulations. In the thin beam limit, the TBT model should give the same results as the EBT. However, due to the use of equal lower-order (i.e., linear) approximations for the displacements and rotation, the element fails to realize the thin beam limit and thus experiences shear locking. Most studies in literature make use of equi-spaced Lagrange higher-order expansions for studying the bending response of plates by Arciniega [5]

* *E-mail address*: *ranrakesh@gmail.com.*

and the same can be extended in one-dimension to study the bending behavior of TBT. The equi-spaced Lagrange interpolation suffers from severe ill-conditioning and for high values of the polynomial degree p [6]. At high p-levels, the discrete problem suffers from a very high condition number of the stiffness matrix and the problem exhibits poor convergence behavior. Very strong preconditioners are recommended in some cases to parse the discrete problem at such high p-levels but the convergence is problem dependent and also dependent on the regularity of the mesh. There has been increased interest in the past decade on using orthogonality of Legendre polynomials to better predict the response of beams when subject to dynamic loadings [7].

The choice of higher-order approximation functions has a dramatic effect on the conditioning of the discrete problem. Significant amount of work has been done to improve higher-order finite elements or p-version FEM [8]. When higher-order approximation functions are used, it is common to examine the condition number of the coefficient matrix generated [9]. The condition number for the mass matrix of the equi-spaced pth degree Lagrange polynomials grows as 10^p whereas the condition number for the Legendre polynomial expansions grows as O(p) [6,9]. The superior conditioning of both the mass and stiffness matrices produced with the Gauss-Lobatto-Legendre functions has been demonstrated by Melenk, et al. [8]. The paper by Maitre, et al. [9] provides the condition numbers of the Legendre expansions to a polynomial order of 30 in two dimensions and 9 in three dimensions. The Lagrange polynomials associated with equi-spaced nodes suffer from linear dependence and special techniques have to be used to address the locking problem. When the beam is thin most of the energy of deformation is due to bending [10]. This problem is commonly treated by reduced integration techniques, although other remedies may be found [1,11]. Shear locking is evident in the weak-form displacement finite element models with equal-order interpolation of the generalized displacements. The phenomenon is more predominant when the length-to-thickness ratio of the beam is high. Higher-order elements have been explored in literature to alleviate shear locking but they have been mostly based on equi-spaced Lagrange polynomials. The use of spectral/*hp* nodal expansions was explored by Pontaza and Reddy [12], who used the least-squares finite element formulation of the linear, first-order shear deformation plate theory. Thus, there have been attempts in the past to alleviate the problems of shear and membrane locking in both beams and plate problems. However, there has not been a uniform method proposing that can solve these locking issues.

In this work, we propose an elegant solution to locking issues with the usage of hp/spectral basis that simultaneously provide spectrally accurate results. The issue of locking has been addressed using two different ways: we use *hp*-spectral approximation functions within the framework of displacement formulations; and secondly we utilize mixed formulations. The motivation for this study comes from the many advantages that are associated with *hp*-higher order elements; spectral convergence (accuracy) of the solutions avoidance of locking, and the orthogonality property of nodal expansions which provide excellent results. Different length-to-thickness, *a/h*, ratios are explored and with appropriate *hp*-refinements full integration is found to provide consistently good agreement with published results for both linear and non-linear analysis.

2 BEAM THEORIES

The EBT theory is based on the assumption that a straight line transverse to the axis of the beam remains straight, inextensible, and normal to the mid-plane after deformation. These assumptions amount to neglecting the Poisson effect and the transverse strains. The displacement field for beams with moderately large rotations but with small strains can be derived using the displacement field

$$u_1(x,z) = u_0(x) - z\frac{\mathrm{d}w_0}{\mathrm{d}x}, \qquad u_2(x,z) = 0, \qquad u_3(x,z) = w_0(x) \tag{1}$$

where (u_1,u_2,u_3) denote the total displacements along the three coordinate directions (x,y,z), and u_0 and w_0 denote the axial and transverse displacements of a point on the neutral axis. The only nonzero *von Karman* non-linear strain is given by

$$\varepsilon_{xx} = \frac{\mathrm{d}u_0}{\mathrm{d}x} + \frac{1}{2}\left(\frac{\mathrm{d}w_0}{\mathrm{d}x}\right)^2 - z\frac{\mathrm{d}^2 w_0}{\mathrm{d}x^2} \tag{2}$$

The Euler-Langrange equations for the EBT can be derived based on the principle of virtual work or the equilibrium of the forces and moments on a typical beam element. For details on the virtual work principle the reader is referred to Reddy [1]. Based on the virtual work principle and separating the virtual displacements we obtain the Euler-Lagrange equations for the EBT as follows:

$$\frac{\mathrm{d}N}{\mathrm{d}x}+f=0, \qquad \frac{\mathrm{d}Q}{\mathrm{d}x}+\frac{\mathrm{d}}{\mathrm{d}x}\left(N\frac{\mathrm{d}w_0}{\mathrm{d}x}\right)+q=0, \qquad \frac{\mathrm{d}M}{\mathrm{d}x}-Q=0 \tag{3}$$

where f is the distributed axial load, q is the distributed transverse load, N is the axial force measured per unit length, and M is the moment measured per unit length

$$N=\int_A \sigma_{xx}\mathrm{d}A, \qquad M=\int_A z\sigma_{xx}\mathrm{d}A \tag{4}$$

And Q is related to M by the third equation in Eq. (3). Assuming a linearly elastic behavior of the material, the relationship between the stress resultants and the displacements can be expressed as

$$N=A_{xx}\left[\frac{\mathrm{d}u_0}{\mathrm{d}x}+\frac{1}{2}\left(\frac{\mathrm{d}w_0}{\mathrm{d}x}\right)^2\right] \tag{5}$$

$$M=-D_{xx}\frac{\mathrm{d}^2w_0}{\mathrm{d}x^2} \tag{6}$$

where

$$(A_{xx},D_{xx})=\int_A E(1,z^2)\,\mathrm{d}A=(EA,EI) \tag{7}$$

The Timoshenko beam theory relaxes the normality restriction of the Euler-Bernoulli beam theory and allows for arbitrary but constant rotation of the transverse normals [1, 13]. The displacement field of the Timoshenko beam theory is given by

$$u_1(x,z)=u_0(x)+z\varphi_x, \qquad u_2(x,z)=0, \qquad u_3(x,z)=w_0(x) \tag{8}$$

where φ_x is the rotation of a transverse normal about the y axis. The equations of equilibrium of the Timoshenko beam theory are the same as those in Eq. (3). The stress resultant N is the same as that defined in Eq. (5), M is given by

$$M=D_{xx}\frac{\mathrm{d}\varphi_x}{\mathrm{d}x} \tag{9}$$

The shear force Q is defined by

$$Q_x=K_s\int_A \sigma_{xx}\mathrm{d}A=S_{xx}\left(\frac{\partial w_0}{\partial x}+\varphi_x\right) \tag{10}$$

Here, K_s denotes the shear correction factor, the value of which is taken as 5/6; S_{xx} is denotes the shear stiffness of the beam

$$S_{xx}=K_s\int_A G\mathrm{d}A=K_sGA \tag{11}$$

where G is the shear modulus and A is the beam cross-sectional area. The non-linearity in both theories comes from the *von-Karman* non-linear strain in Eq. (2). For a complete treatment of the EBT and TBT with the displacement based formulations and the derivation of the weak forms, the reader is referred to Reddy [1].

3 GOVERNING EQUATIONS OF EBT

The governing equations of the Euler-Bernoulli beam theory can be expressed in several forms using different variables, and different finite element models can be developed. We derive the governing equations for the EBT from the principle of virtual work. The principle states that if a body is under equilibrium the total virtual work done by actual internal and external forces in moving through their respective displacements is zero. For the beam problem it is stated as

$$\delta W = \delta W_I^e - \delta W_E^e \tag{12}$$

δW_I^e is the virtual strain energy in moving a body due to actual stresses σ_{ij} in moving through the virtual strains $\delta\varepsilon_{ij}$ and δW_E^e is the virtual work done by externally applied loads. For the beam element we obtain the equations as follows;

$$\delta W = \int_{V^e} \delta\varepsilon_{ij}\sigma_{ij}\mathrm{d}A - \int_{x_a}^{x_b} q\delta w_0 \mathrm{d}x - \int_{x_a}^{x_b} f\delta u_0 \mathrm{d}x \tag{13}$$

Following through with the stresses and strains in the expression for the virtual strain energy we obtain

$$\begin{aligned}
\delta W = \delta W_I^e - \delta W_E^e &= \int_{V^e} \delta\varepsilon_{xx}\sigma_{xx}\mathrm{d}A\mathrm{d}x = \int_{V^e} (\delta\varepsilon_{xx}^0 + z\delta\varepsilon_{xx}^1)\sigma_{xx}\mathrm{d}A\mathrm{d}x \\
&= \int_{V^e} \left[\left(\frac{\mathrm{d}\delta u_0}{\mathrm{d}x} + \frac{\mathrm{d}w_0}{\mathrm{d}x}\frac{\mathrm{d}\delta w_0}{\mathrm{d}x} \right) N_{xx} - z\frac{\mathrm{d}^2\delta w_0}{\mathrm{d}^2 x} \right] \sigma_{xx}\mathrm{d}A\mathrm{d}x \\
&= \int_{V^e} \left[\left(\frac{\mathrm{d}\delta u_0}{\mathrm{d}x} + \frac{\mathrm{d}w_0}{\mathrm{d}x}\frac{\mathrm{d}\delta w_0}{\mathrm{d}x} \right) N_{xx} - z\frac{\mathrm{d}^2\delta w_0}{\mathrm{d}^2 x} M_{xx} \right] \mathrm{d}x - \int_{x_a}^{x_b} q\delta w_0 \mathrm{d}x - \int_{x_a}^{x_b} f\delta u_0 \mathrm{d}x
\end{aligned} \tag{14}$$

Separating the variations of δu_0 and δw_0 we obtain the Euler-Lagrange equations for the EBT

$$\begin{aligned}
\delta u_0 : \quad & -\frac{\mathrm{d}N_{xx}}{\mathrm{d}x} = f(x) \\
\delta w_0 : \quad & -\frac{\mathrm{d}}{\mathrm{d}x}\left(\frac{\mathrm{d}w_0}{\mathrm{d}x} N_{xx} \right) - \frac{\mathrm{d}^2 M_{xx}}{\mathrm{d}x^2} = q(x)
\end{aligned} \tag{15}$$

The above equations can be decomposed into the following equations for the first mixed model:

$$\frac{\mathrm{d}N}{\mathrm{d}x} + f = 0 \tag{16}$$

$$\frac{\mathrm{d}}{\mathrm{d}x}\left(\frac{\mathrm{d}M}{\mathrm{d}x} + N\frac{\mathrm{d}w_0}{\mathrm{d}x} \right) + q = 0 \tag{17}$$

$$N = A_{xx}\left[\frac{\mathrm{d}u_0}{\mathrm{d}x} + \frac{1}{2}\left(\frac{\mathrm{d}w_0}{\mathrm{d}x} \right)^2 \right] \tag{18}$$

$$M = -D_{xx}\frac{\mathrm{d}^2 w_0}{\mathrm{d}x^2} \tag{19}$$

The development of the weak finite element models for the equations follows multiplication of the above with weight function and integration by parts. Assigning the variables in the formulation in the order: [u_j, w_j, N_j, M_j]. The primary (PV) and secondary variables (SV) are as follows:

$$\text{PVs}: \; u_0,\, w_0,\, \frac{\mathrm{d}w_0}{\mathrm{d}x} \tag{20}$$

$$\text{SVs}: \; N,\, V,\, M \tag{21}$$

where V is the equivalent shear force,

$$V = Q + N\frac{\mathrm{d}w_0}{\mathrm{d}x} \tag{22}$$

The above classification of the primary and secondary variables is instructive in determining the appropriate boundary conditions that should be applicable. Although, the deflection and the derivative of the deflection have been mentioned as the primary variables it should be noted that since we are not dealing with a displacement based formulation the formulation admits C^0 continuity as minimally confirming. Based on the equations that were presented above the shear force is absorbed into the formulation and there are four variables per node, for this mixed model, namely axial displacement u_x, the deflection w_x, shear force N_{xx}, and the moment M_{xx}. For the second mixed model considered for analysis, the equations are kept in their primitive forms and the resulting formulation has six degrees of freedom per node. The governing differential equations presented above are modified thus (repeated for clarity):

$$\frac{\partial N_{xx}}{\partial x} + f_x = 0 \tag{23}$$

$$\frac{\partial V_{xx}}{\partial x} + q_x = 0 \tag{24}$$

$$\frac{\partial M_{xx}}{\partial x} - V + N_{xx}\frac{\partial w_0}{\partial x} = 0 \tag{25}$$

$$N_{xx} = EA\left[\frac{\partial u_0}{\partial x} + \frac{1}{2}\left(\frac{\partial w_0}{\partial x}\right)^2\right] \tag{26}$$

$$M_{xx} = -EI\frac{\partial^2 w_0}{\partial x^2} \tag{27}$$

The primary and secondary variables have already been defined earlier. The finite element formulation follows the standard procedures as detailed earlier. The order of the variables for the generation of the stiffness matrix coefficients are [u_i, w_i, θ_i, N_i, V_i, M_i].

4 GOVERNING EQUATIONS OF TBT

Displacement based formula seeks to find the solution of the governing equations with all the equations expressed in terms of the displacements, that define the displacement based TBT theory. The derivation of Euler-Lagrange equations for the TBT theory follows from the principle of virtual work completely analogously to EBT.

$$-\frac{\partial}{\partial x}\left[A_{xx}\left\{\frac{\partial u_0}{\partial x}+\frac{1}{2}\left(\frac{\partial w_0}{\partial x}\right)^2\right\}\right]=f \tag{28}$$

$$-\frac{\partial}{\partial x}\left[S_{xx}\left\{\phi_x+\frac{\partial w_0}{\partial x}\right\}\right]-\frac{\partial}{\partial x}\left[A_{xx}\frac{\partial w_0}{\partial x}\left\{\frac{\partial u_0}{\partial x}+\frac{1}{2}\left(\frac{\partial w_0}{\partial x}\right)^2\right\}\right]=q \tag{29}$$

$$S_{xx}\left\{\phi_x+\frac{\partial w_0}{\partial x}\right\}-\frac{\partial}{\partial x}\left[D_{xx}\frac{\partial \phi_x}{\partial x}\right]=0 \tag{30}$$

The primary (PV) and the secondary variables (SV) include the specification of either the displacements or forces as follows:

$$\text{PV}:\ u_0,\ w_0,\ \phi_x \tag{31}$$

$$\text{SV}:\ N_{xx},\ Q_x,\ M_{xx} \tag{32}$$

The above equations describe the bending response of TBT, where, v is Poisson ratio for the isotropic beam under consideration. The finite element equations for the displacement based formulation have been outlined in [1] and have been omitted here in the interest of brevity. Mixed formulation for the Timoshenko beam theory starts with the same equations as the displacement based formulations but the equations are kept in primitive variables with no substitutions to bring every equation in terms of displacements. The equations that comprise the finite element formulation are being (repeated here) for clarity.

$$\frac{\partial N_{xx}}{\partial x}+f_x=0 \tag{33}$$

$$\frac{\partial M_{xx}}{\partial x}-Q_x=0 \tag{34}$$

$$\frac{\partial Q_{xx}}{\partial x}+\frac{\partial}{\partial x}\left(N_{xx}\frac{\partial w_0}{\partial x}\right)+q=0 \tag{35}$$

$$N_{xx}=EA\left[\frac{\partial u_0}{\partial x}+\frac{1}{2}\left(\frac{\partial w_0}{\partial x}\right)^2\right] \tag{36}$$

$$M_{xx}=EI\frac{\partial \phi_x}{\partial x} \tag{37}$$

$$Q_x=S_{xx}\left[\frac{\partial w_0}{\partial x}+\phi_x\right] \tag{38}$$

The order of variables for the generation of the stiffness matrix coefficients are [u_i, w_i, θ_i, N_i, V_i, M_i].

5 SPECTRAL/HP ELEMENT FORMULATION

The spectral finite element approximation is stated as follows, the primary variables are each approximated as

$$\Delta^e=\sum_{j=1}^{n}\Delta_j\psi_j \tag{39}$$

where, ψ_j are the nodal expansions, which are provided by the following one-dimensional C^0 spectral nodal basis;

$$\psi_j = \frac{(\varsigma-1)(\varsigma+1)L_p^{'}(\varsigma)}{p(p+1)L_p(\varsigma_i)(\varsigma-\varsigma_p)} \tag{40}$$

where, Δ_j are the nodal values due to the Kronecker delta property of the spectral basis. L_p=$P_p^{(0,0)}$ is the Legendre polynomial of order p, and ζ_i denotes the location of the roots of $(\zeta\text{-}1)(\zeta\text{+}1)L_p^{'}(\zeta)=0$ in the interval [-1,+1]. All Jacobi polynomials, $P_n^{\alpha,\beta}$, satisfy a three-term recurrence relation of the form:

$$xP_n^{\alpha,\beta} = a_{n,-1,n}^{\alpha,\beta}P_{n-1}^{\alpha,\beta}(x) + a_{n,n}^{\alpha,\beta}P_n^{\alpha,\beta}(x) + a_{n+1,n}^{\alpha,\beta}P_{n+1}^{\alpha,\beta}(x) \tag{41}$$

where, $a^{\alpha,\beta}$ only depends on α, β, and n. And the derivatives of Jacobi polynomials satisfy a three-term recurrence relation of the form [14, 15];

$$xP_n^{\alpha,\beta} = a_{n,-1,n}^{\alpha,\beta}P_{n-1}^{\alpha,\beta}(x) + a_{n+1,n}^{\alpha,\beta}P_{n+1}^{\alpha,\beta}(x) \tag{42}$$

For the special case of α, β=1, we drop the superscript and the above equation can be written as:

$$xP_n = a_1(n)P_{n-1}(x) + a_2(n)P_{n+1}(x) \tag{43}$$

where

$$a_1(n) = \frac{n+1}{2n+3} \tag{44}$$

and

$$a_2(n) = \frac{(n+1)(n+3)}{(2n+1)(2n+3)} \tag{45}$$

All Jacobi polynomials satisfy the three terms recurrence relationship of the form

$$(1-x^2)\frac{\mathrm{d}P_n^{\alpha,\beta}}{\mathrm{d}x} = c_{n-1,n}^{\alpha,\beta}(n)P_{n-1}^{\alpha,\beta}(x) + c_{n+1,n}^{\alpha,\beta}(n)P_{n-1}^{\alpha,\beta}(x) \tag{46}$$

Seeking the recurrence relation for the derivative, we rewrite the above equation by dropping α, and β, for the special case of α, β=1

$$(1-x^2)\frac{\mathrm{d}P_n}{\mathrm{d}x} = c_1(n)P_{n-1}(x) + c_2(n)P_{n+!}(x) \tag{47}$$

where

$$c_1(n) = \frac{(n+1)(n+3)}{2n+3} \tag{48}$$

and

$$c_2(n) = \frac{2n(n+1)(n+3)}{(2n+3)(2n+4)} \tag{49}$$

For an illustration of the proofs of these above mentioned equalities see Osilenker [14].

6 LINEARIZATION PROCEDURE

The linearization process can be accomplished with either of two techniques, namely the Picard (direct iteration procedure) or the Newton-Raphson's method. For checking the convergence behavior of both the methods of linearization with *hp*-spectral methods both of these were implemented. Some of the advantages of the Newton-Raphson method are a faster convergence rate, since we are using incremental load steps for the runs. The linearized problem with the Newton's method is represented as follows:

$$\left[K^e\left\{\Delta^e\right\}^r\right]^{\tan}\left\{\delta\Delta\right\}^e=-\left\{R^e\right\}^r \tag{50}$$

The linear convergence criterion was set at a reduction in the L^2 norm of the residuals to a tolerance value of 10^{-06}, whereas the non-linear convergence was declared when L^2 norm of the incremental vector normalized with the norm of the solution vector was less than 10^{-03} for the displacement based FEM models. The mixed FEM models were solved with Gaussian Elimination with scaled partial pivoting. In the forthcoming sections, we present the results that we obtained for the linear and non-linear problems that were studied with different types of boundary conditions and also verify the spectral convergence of the solutions in the L^2 norm.

7 BOUNDARY CONDITIONS

The specification of the boundary condition for the beam problem can be specified based on a number of different ways in which the beam is supported. The different boundary conditions that were examined were the clamped-clamped, pinned-pinned, and the hinged-hinged case. The clamped-clamped case involves the specification of the following variables to zero

$$u=w_0=\varphi_x=0 \tag{51}$$

The pinned-pinned case requires the specification of the following variables to be zero

$$u=w_0=0 \tag{52}$$

Also, the specification of the third variable comes from the specification of the end moment, which is zero for the case that the ends are not subject to any external moments. For the displacement based formulation the following is satisfied in an integral sense, and no special treatment to the right hand side of the vector needs to be done. For the mixed based formulations, the same is specified explicitly. Finally, the hinged-hinged case involves the specification of the following variables:

$$w_0=0 \tag{53}$$

Also, following this analysis two other variables, namely N_{xx}, and M_{xx} are zero. Different *a/h* ratios were explored for both the models, subject to different boundary conditions.

8 NUMERICAL RESULTS

The TBT beam was solved with the displacement based formulation and the mixed formulation where as the EBT beam was solved with mixed finite element formulation.

8.1 Linear series solutions

Analytical solutions for the Timoshenko beam theory as also the first order shear deformation theory of plates exist in terms of the Navier solutions in two dimensions. For a complete description of the Navier equations, the reader is

referred to Reddy [16, 17]. The solution to the problem can be expressed in terms of an infinite series which can be extended to any desired level of accuracy with the help of inclusion of an appropriate number of terms in the infinite expansion. The boundary conditions of simply supported beams are expressed as [17]: w=0 and M=0, at x=0,L. The following expressions of the generalized displacements w, and φ_x satisfy the boundary conditions for the EBT;

$$w(x,t)=\sum_{n=1}^{\infty}W_n \sin(\frac{n\pi x}{L})\ \mathrm{e}^{\mathrm{i}\omega_n t} \tag{54}$$

$$\varphi(x,t)=\sum_{n=1}^{\infty}\varphi_n \cos(\frac{n\pi x}{L})\ \mathrm{e}^{\mathrm{i}\omega_n t} \tag{55}$$

The term φ_x has the meaning of derivative of the deflection at that location for the Euler-Bernoulli beam theory whereas the Timoshenko beam theory admits an independent slope which gets added to the transverse shear term to generate the total slope of the beam. For static bending, we set all the time derivatives to zero and take the distributed load to be of the form;

$$q(x)=\sum_{n=1}^{\infty}Q_n \sin(\frac{n\pi x}{L}) \tag{56}$$

$$Q_n=\frac{2}{L}\int_0^L q(x)\sin\left(\frac{n\pi x}{L}\right)\mathrm{d}x \tag{57}$$

The coefficients Q_n associated with uniform load is obtained as follows [17] $q(x)=q_0$

$$Q_n=\frac{4q_0}{n\pi} \tag{58}$$

Substituting the expansions for w, φ, and $q(x)$ into the governing differential equations for the Euler-Bernoulli beam theory we obtain the following expressions for the deflection and slope for the Euler-Bernoulli beam undergoing linear bending deformations [16];

$$w(x)=\sum_{n=1}^{\infty}\lambda_n\frac{Q_n L^4}{n^4\pi^4 EI}\sin\left(\frac{n\pi x}{L}\right) \tag{59}$$

$$\phi(x)=\sum_{n=1}^{\infty}\lambda_n\frac{Q_n L^3}{n^3\pi^3 EI}\cos\left(\frac{n\pi x}{L}\right) \tag{60}$$

where the non-local parameter λ_n has the effect of increasing the deflection. The definition of λ_n follows

$$\lambda_n=\left(1+\mu\frac{n^2\pi^2}{L^2}\right) \tag{61}$$

The linear solution that corresponds to the solution of the Timoshenko Beam Theory are provided next. Consider a Timoshenko beam subject to the same boundary conditions as mentioned earlier for the EBT beam for linear analysis. For the case that the beam is subject to a uniform load the final expressions for the deflections and slopes for the Timoshenko beam elements are:

$$w(x)=\sum_{n=1}^{\infty}\lambda_n\Delta_n\frac{Q_n L^4}{n^4\pi^4 EI}\sin\left(\frac{n\pi x}{L}\right) \tag{62}$$

$$\phi(x)=\sum_{n=1}^{\infty}\lambda_n\frac{Q_n L^3}{n^3\pi^3 EI}\cos\left(\frac{n\pi x}{L}\right) \tag{63}$$

where the constants introduced are defined as follows:

$$\lambda_n = (1 + n^2\pi^2\Omega), \qquad \Omega = \frac{EI}{GAK_s L^2} \tag{64}$$

The linear series solutions provided above serve as a very good estimate to the actual results obtained from the solutions of the different beam theories mentioned both to serve as validation benchmarks for the problems solved and also to provide checks on the exponential convergence of the errors in the L^2 norms.

9 NONLINEAR SOLUTIONS

The first formulation studied is the displacement based formulation, and the second formulation is the mixed formulation. Both of these will be described in the following sections for both beam theories studied.

10 EULER-BERNOULLI BEAM THEORY

Results from finite element mixed model I and FE mixed II are both discussed in the following sections.

10.1 Hinged-hinged B.C. (EBT)

Consider a EBT beam which is subject to hinged-hinged boundary conditions at both ends. The beam length L=100 in., 1 in × 1in crossection, made of steel (E=30 msi), and subjected to a uniform loading of intensity q_0 lb/in. The Poisson ratio for the beam was taken as 0.25. For mixed model I the whole domain of the beam was modeled. The geometric boundary conditions for the beam hinged-hinged boundary condition has been specified earlier. The non-dimensionalization of the deflection was carried out based on equation [65]. A total of 10 elements were used for this analysis, with uniformly spaced levels and uniform p_{level}. The discrete problem resulted in a total of 124 degrees of freedom of the system. A constant p_{value} of 3 was used in each element. The uniform load parameter of 1.0 was used for stepping through the loads till a maximum value of 10 (as reported in Table 1) was reached. For the mixed model II ,ten elements were used in the analysis with a p_{value} of 7. A relatively high p_{level} was used for this analysis. For the mixed formulation II ,each node has a total of six degrees of freedom. The discrete problem consisted of a total of 426 degrees of freedom. As can be seen from Table 1 the agreement with the *hp*-spectral results and the results of Reddy [1] is excellent. The maximum percentage error between the mixed model II and the reduced integration results of Reddy [1] was found to be 0.004%. Hinged-hinged case is the most sensitive case for checking locking issues and it was realized that with appropriate p_{level} refinement there was no need to use reduced integration to obtain excellent results.

10.2 Pinned-pinned B.C. (EBT)

Consider a beam with the material properties defined earlier subject to pinned-pinned boundary condition. Newton's method of linearization was used to obtain the results.

Table 1
Hinged-Hinged case results EBT models

$q(xx)$	Mixed Model I (MX1)		Mixed Model II (MX II)		Reddy (04)
	w_0	w (dimlss)	w_0	w (dimlss)	w_0
1	0.5208	1.3020	0.5208	1.3020	0.5208
2	1.0416	2.6041	1.0416	2.6041	1.0417
3	1.5625	3.9062	1.5625	3.9062	1.5625
4	2.0833	5.2083	2.0833	5.2083	2.0833
5	2.6041	6.5104	2.6041	6.5104	2.6042
6	3.125	7.8125	3.1250	7.8125	3.125
7	3.6458	9.1145	3.6458	9.1145	3.645
8	4.1666	10.4166	4.1666	10.4166	4.1667
9	4.6875	11.7187	4.6875	11.7187	4.6875
10	5.2083	13.0208	5.2083	13.0208	5.2083

Table 2
Pinned-pinned case results EBT models

$q(xx)$	Mixed Model I (MX I)		Mixed Model II (MX II)		Reddy (04)
	w_0	w (dimlss)	w_0	w (dimlss)	w_0
1	0.3697	0.9244	0.3685	0.9212	0.3685
2	0.5478	1.3696	0.5454	1.3636	0.5454
3	0.6675	1.6687	0.6643	1.6607	0.6640
4	0.7593	1.8983	0.7556	1.8891	0.7555
5	0.8353	2.0884	0.8313	2.0783	0.8312
6	0.9008	2.2521	0.8964	2.2412	0.8964
7	0.9586	2.3966	0.9540	2.3851	0.9540
8	1.0107	2.5267	1.0059	2.5147	1.0058
9	1.0582	2.6455	1.0532	2.6330	1.0531
10	1.1020	2.7550	1.0968	2.7421	1.0967

Table 3
Pinned-pinned results for different *a/h* ratios (EBT)

$q(xx)$	Non-dimensional displacements different a/h ratios			
	w_{10}	w_{20}	w_{25}	w_{100}
1	1.3020	1.3020	1.3020	0.9213
2	2.6041	2.6041	2.6040	1.3637
3	3.9062	3.9061	3.9058	1.6609
4	5.2083	5.2081	5.2072	1.8893
5	6.5104	6.5100	6.5083	2.0785
6	7.8124	7.8119	7.8089	2.2414
7	9.1145	9.1136	9.1090	2.3854
8	10.4166	10.4152	10.4083	2.5150
9	11.7187	11.7167	11.7068	2.6332
10	13.0208	13.0180	13.0045	2.7423

Table 4
Clamped-Clamped case results EBT models

$q(xx)$	Mixed Model I (MX I)		Mixed Model II (MX II)		Reddy (04)
	w_0	w (dimlss)	w_0	w (dimlss)	w_0
1	0.1033	0.2584	0.1033	0.2584	0.1035
2	0.2024	0.5061	0.2023	0.5057	0.2025
3	0.2944	0.7361	0.2940	0.7350	0.2943
4	0.3784	0.9460	0.3775	0.9438	0.3777
5	0.4545	1.1364	0.4531	1.1329	0.4534
6	0.5237	1.3092	0.5218	1.3045	0.5220
7	0.5867	1.4669	0.5843	1.4608	0.5845
8	0.6445	1.6114	0.6416	1.6040	0.6418
9	0.6979	1.7449	0.6945	1.7362	0.6946
10	0.7474	1.8687	0.7435	1.8588	0.7436

The non-dimensional deflections at the center of the beam are also being reported for this beam in Table 2. A total of 10 elements were used for Mixed Model I, with gradation at the edges of the beam as explained earlier. The discrete problem resulted in a total of 124 degrees of freedom of the system. A constant p_{value} of 3 was used in each element. The uniform load parameter of 1.0 was used for stepping through the loads till a maximum value of 10 (as reported in Table 2) was reached. For the mixed finite element formulations for the Euler-Bernoulli beam models a higher value of p_{value} was used in some cases (as illustrated later) to resolve the stresses and moments to a high level of accuracy. For mixed model II twenty elements were used in the analysis with a p_{level} of 9. For the mixed formulation each node has a total of six degrees of freedom. The discrete problem consisted of a total of 1086 degrees of freedom. Reddy [1] results were obtained with 4 quadratic elements with reduced integration techniques for this case. The maximum percentage error between the two different mixed models was found to be 0.5%. The non-dimensional deflections for the different *a/h* ratios for the pinned-pinned cases were also explored and are presented in Table 3.

10.3 Clamped-clamped B.C. (EBT)

Consider a beam which is subjected to clamped-clamped boundary conditions at both ends. The beam length L=100 in., 1 in × 1 in crossection, made of steel (E=30 msi), and subject to a uniform loading of intensity q_0 lb/in. The Poisson ratio for the beam was taken as 0.25. Table 4. reports the deflections of the center of the beam subject to the clamped-clamped boundary condition and also the non-dimensional deflections at the center of the beam.

A total of 10 elements were used for this analysis for mixed model I, with uniform elements with a uniform p_{level} in each element. The discrete problem resulted in a total of 204 degrees of freedom of the system. A constant p value of 5 was used in each element. The uniform load parameter of 1.0 was used for stepping through the loads till a maximum value of 10 (as reported in Table 4) was reached. A high value of p_{level} was used in certain cases to generate more confidence in the results. The discrete problem was solved with Gaussian-Elimination with scaled partial pivoting. The results presented above is for the case where a/h=100. The maximum percentage error between the two models was found to be 0.52%. Different a/h ratios were analyzed and Table 5. reports the non-dimensionalized center deflection as a function of the changing length of the beam. For the analysis of the beam deflection with changing lengths of the beam, 10 elements were used, and the full beam was modeled. The p_{level} used was set at a uniform value of 9 to generate these results. The model consisted of a total of 546 degrees of freedom which was stepped with Newton's method. Based on the above observations the non-dimensional load vs. deflection curves for clamped-clamped Euler-Bernoulli beams is constant with varying lengths from a range of a/h=10 through a value of a/h=75 and varies significantly only for the case of a slender beam of slenderness ratio a/h=100.

11 TIMOSHENKO BEAM THEORY

Non-linear results obtained with the solutions of the Timoshenko beam theory with the displacement (DX) and the mixed formulation (MX) have been outlined with published results in literature.

Table 5
Clamped-Clamped results for different a/h ratios (EBT)

q(xx)	Non-dimensional displacements different a/h ratios			
	w_{10}	w_{20}	w_{25}	w_{100}
1	0.2604	0.2604	0.2604	0.2584
2	0.5208	0.5208	0.5208	0.5057
3	0.7812	0.7812	0.7812	0.7350
4	1.0416	1.0416	1.0416	0.9438
5	1.3020	1.3020	1.3020	1.1329
6	1.5624	1.5624	1.5624	1.3045
7	1.8229	1.8229	1.8229	1.4608
8	2.0833	2.0833	2.0833	1.6040
9	2.3437	2.3437	2.3437	1.7362
10	2.6041	2.6041	2.6041	1.8588

Table 6
Hinged-Hinged case results TBT models

$q(xx)$	Displacement (DX)		Mixed (MX)		Reddy (04)
	w_0	w (dimlss)	w_0	w (dimlss)	w_0
1	0.5209	1.3024	0.5209	1.3023	0.5208
2	1.0386	2.5966	1.0419	2.6047	1.0417
3	1.5629	3.9072	1.5628	3.9071	1.5625
4	2.0838	5.2096	2.0838	5.2095	2.0833
5	2.6048	6.5119	2.6047	6.5119	2.6042
6	3.1258	7.8144	3.1257	7.8143	3.1250
7	3.6467	9.1167	3.6467	9.1167	3.6458
8	4.1677	10.419	4.1676	10.4191	4.1667
9	4.6887	11.722	4.6886	11.7215	4.6875
10	5.2096	13.024	5.2095	13.0239	5.2083

11.1 Hinged-hinged B.C. (TBT)

Consider a beam which is subjected to hinged-hinged boundary conditions at both ends. The beam length L=100 in., 1×1 in^2 cross section, made of steel E=30 msi, subject to a uniform loading of intensity q_0 lb/in. The Poisson ratio for the beam was taken as 0.25. The non-dimensionalization of the deflection was carried out based on the following formula;

$$w = \frac{100 * w_{\max} * D_{xx}}{L^4} \tag{65}$$

Also, the results obtained in the above cited reference were obtained using reduced integration techniques whereas we propose the useage of *full integration* with appropriate hp-refinements. The non-dimensional deflections at the center of the beam are also being reported for this beam in Table 6. A total of 10 elements were used for this analysis, with gradation at the edges of the beam to capture the development of strain and stress concentrations at the end of the beam (boundary layers). The gradation of half beam is being presented below

$$\Delta(x) = \{0.25,\ 0.25,\ 0.25,\ 0.25,\ 4.0,\ 9.0,\ 9.0,\ 9.0,\ 9.0,\ 9.0\} \tag{66}$$

The discrete problem resulted in a total of 153 degrees of freedom of the system for the displacement based formulation. A constant p_{value} of 5 was used in each element. The uniform load parameter of 0.50 was used for stepping through the loads till a maximum value of 10 (as reported in Table 1) was reached. For the mixed formulation since, the shear forces and the moments at the center of the beam are not known the full beam was modeled. Ten elements were used in the analysis with a p_{value} of 14. For the mixed formulation each node has a total of six degrees of freedom. The discrete problem consisted of a total of 846 degrees of freedom. As can be seen from Table 6 the agreement with the *hp*-spectral results and reported results of Reddy [1] is excellent. The maximum error between the mixed and displacement model results was found to be 0.32%.

11.2 Pinned-pinned boundary condition (TBT)

Consider a TBT beam with material properties defined earlier subject to pinned-pinned boundary condition. The non-dimensional deflections at the center of the beam are also being reported for this beam in Table 7. Reddy results were obtained with 4 quadratic elements at with reduced integration techniques for this case. A total of 10 elements were used for this analysis, with gradation at the edges of the beam. The discrete problem resulted in a total of 183 degrees of freedom of the system for the displacement based formulation. A constant p_{value} of 6 was used in each element. The uniform load parameter of 0.50 was used for stepping through the loads till a maximum value of 10 (as reported in Table 2) was reached. For the mixed finite element formulations for the Timoshenko beam models a higher value of p was used in some cases to generate more confidence in the results and also to resolve the stresses and moments to a high level of accuracy. As can be seen from Table 7. the agreement of the *hp*-spectral results and the results of Reddy [1] is excellent. The maximum error between the mixed and displacement model results was found to be 1.56%. The non-dimensional deflections for the different a/h ratios for the pinned-pinned cases were also explored and have been presented in Table 8.

Table 7
Pinned-pinned case results TBT models

$q(xx)$	Displacement (DX)		Mixed (MX)		Reddy (04)
	w_0	w (dimlss)	w_0	w (dimlss)	w_0
1	0.3685	0.9212	0.3693	0.9234	0.3685
2	0.5454	1.3636	0.5467	1.3669	0.5454
3	0.6645	1.6614	0.6655	1.6638	0.6640
4	0.7556	1.8891	0.7536	1.8841	0.7555
5	0.8312	2.0781	0.8316	2.0790	0.8312
6	0.8963	2.2409	0.8993	2.2483	0.8964
7	0.9539	2.3848	0.9588	2.3970	0.9540
8	1.0058	2.5144	1.0205	2.5514	1.0058
9	1.0531	2.6327	1.0525	2.6312	1.0531
10	1.0967	2.7417	1.1139	2.7849	1.0967

Table 8
Pinned-pinned results for different *a*/*h* ratios (TBT)

a(*xx*)	Non-dimensional displacements different *a*/*h* ratios			
	w_{10}	w_{20}	w_{25}	w_{100}
1	1.3333	1.3099	1.3071	0.9212
2	2.6667	2.6198	2.6140	1.3636
3	4.0000	3.9296	3.9208	1.6614
4	5.3333	5.2394	5.2273	1.8891
5	6.6667	6.5491	6.5333	2.0781
6	8.0000	7.8588	7.8389	2.2409
7	9.3333	9.1683	9.1439	2.3848
8	10.667	10.478	10.448	2.5144
9	12.000	11.787	11.752	2.6327
10	13.333	13.096	13.054	2.7417

Table 9
Clamped-Clamped case results TBT models

q(*xx*)	Displacement (DX)		Mixed (MX)		Reddy (04)
	w_0	*w* (dimlss)	w_0	*w* (dimlss)	w_0
1	0.1034	0.2587	0.1034	0.2587	0.1035
2	0.2025	0.5063	0.2025	0.5063	0.2025
3	0.2942	0.7356	0.2943	0.7358	0.2943
4	0.3777	0.9444	0.3779	0.9449	0.3777
5	0.4533	1.1335	0.4537	1.1343	0.4534
6	0.5219	1.3049	0.5224	1.3061	0.5220
7	0.5843	1.4610	0.5850	1.4626	0.5845
8	0.6416	1.6041	0.6424	1.6061	0.6418
9	0.6944	1.7361	0.6954	1.7385	0.6946
10	0.7434	1.8586	0.7445	1.8613	0.7436

Table 10
Clamped-clamped results for different *a*/*h* ratios

q(*xx*)	Non-dimensional displacements different *a*/*h* ratios			
	w_{10}	w_{20}	w_{25}	w_{100}
1	0.2916	0.2682	0.2654	0.2587
2	0.5833	0.5364	0.5308	0.5064
3	0.8749	0.8046	0.7962	0.7361
4	1.1666	1.0729	1.0616	0.9454
5	1.4583	1.3411	1.3270	1.1351
6	1.7499	1.6093	1.5924	1.3073
7	2.0416	1.8776	1.8579	1.4642
8	2.3333	2.1458	2.1233	1.6080
9	2.6249	2.4140	2.3887	1.7407
10	2.9166	2.6822	2.6541	1.8638

11.3 Clamped-clamped B.C. (TBT)

Consider a beam which is subjected to clamped-clamped boundary conditions at both ends. The beam length L=100 in., 1 × 1 in^2 cross section, made of steel (E=30 msi), and subjected to a uniform loading of intensity q_0 lb/in. The Poisson ratio considered was taken as 0.25. Using the symmetry of the beam around the center of the beam, one half of the beam needed to have been modeled. Table 9. reports the deflections of the center of the beam subjected to the clamped-clamped boundary condition and also the non-dimensional deflections at the center of the beam for both the mixed and displacement based formulations.

Reddy [1] results were obtained with 4 quadratic elements at with reduced integration techniques for this case. A total of 10 elements were used for this analysis, with gradation at the edges of the beam. The discrete problem resulted in a total of 153 degrees of freedom of the system. A constant p_{value} of 5 was used in each element. The uniform load parameter of 0.50 was used for stepping through the loads till a maximum value of 10 was reached. The run presented above is for the case where *a*/*h*=100.

Table 11
Hinged-hinged case results TBT models

$q(xx)$	Mixed p=3		Mixed p=7	
	w_0	w (dimlss)	w_0	w (dimlss)
1	5.209472	1.302368	5.209583	1.302395
2	10.41894	2.604736	10.41916	2.604791
3	15.62842	3.907104	15.62875	3.907187
4	20.83789	5.209472	20.83833	5.209583
5	26.04736	6.51184	26.04791	6.511979
6	31.25683	7.814208	31.25750	7.814374
7	36.46631	9.116576	36.46708	9.116770
8	41.67578	10.41894	41.67666	10.41916
9	46.88525	11.72131	46.88625	11.72156
10	52.09472	13.02368	52.09583	13.02395

As can be seen from Table 9 the agreement of the *hp*-spectral results and the results of Reddy [1] is excellent. The maximum error between the mixed and displacement model results was found to be 0.15%. Different a/h ratios analysis were carried out and Table 10. reports the non-dimensionalized center deflection as a function of the changing length of the beam.

For the analysis of the beam deflection with changing lengths of the beam, 10 elements were used, and the full beam was modeled. The p_{level} used was set at a uniform value of 9 to generate the results. This resulted in a total of 546 degrees of freedom, the nonlinear problem was stepped with Newton's method. As can be seen from the results presented here, an increase in the length of the beam did not cause any deterioration of the results and all the results were obtained with *full integration* techniques.

11.4 Large displacement analysis (TBT)

We consider a beam subject to hinged-hinged boundary conditions studied with TBT undergoing large deflections for testing the robustness of hp/spectral methods for predicting large deflections and the effects of membrane and shear locking. The beam considered has a length of L=100 in., 1×1 in^2 cross section, made of steel E=3 msi, subject to a uniform loading of intensity q_0 lb/in. The Poisson ratio for the beam was taken as 0.25. The non-dimensionalization of the deflection was obtained based on Eq. (65);

The non-dimensional deflections at the center of the beam are also being reported for this beam in Table 11. for p-refinements of 3 and 7 respectively. A total of 10 elements were used which were distributed equally over the length of the beam. The discrete problem resulted in varying degrees of freedom of the system for the mixed formulation which was solved for a range of p-refinements varying from 4 through 7. A constant p_{value} was used in each element even if the p-levels were varied for different cases. The uniform load parameter of 10 was used for stepping through the loads till a maximum value of 100 (as reported in Table 11) was reached. Varying p-levels were tested to solve the problem to obtain grid independent results and the end deflections are presented in Table 11. The fourth decimal place difference in the results between different p-levels tested were used to obtain highly accurate results at the expense of slight increase in the computational effort in solving the larger linear system. It is of interest to note that we performed a series of parametric analysis for solving all the beam problems studied with both low and high p-levels. We have reported values obtained with higher p-levels in order to report highly accurate results. For other problems it is suggested to vary both the h and p refinements for the problems in structural applications.

12 DISCUSSION

There are advantages of the displacement based model over the mixed-models utilized. The displacement based finite element model generates a simpler problem from the matrix inversion point of view as the terms are of the same order in the equation. Mixed model on the other hand have disparate order terms which cause the model to experience significant convergence issues with standard iterative solvers. Direct solvers were found to be able to parse the discrete system.

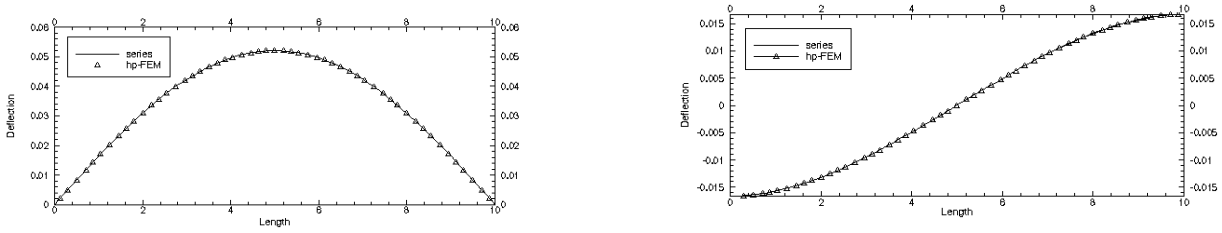

Fig. 1
Agreement between the series solutions for the deflections and the slopes with *hp*-SEM results for the Euler-Bernoulli beam theory.

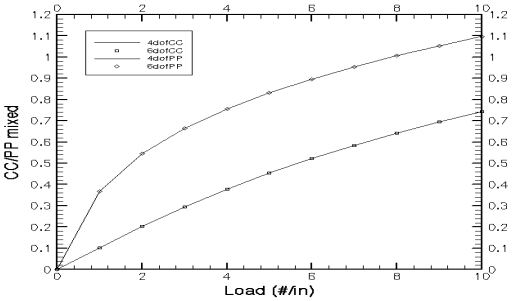

Fig. 2
Load vs. deflection curves for CC/PP boundary conditions mixed/displacement based models for EBT.

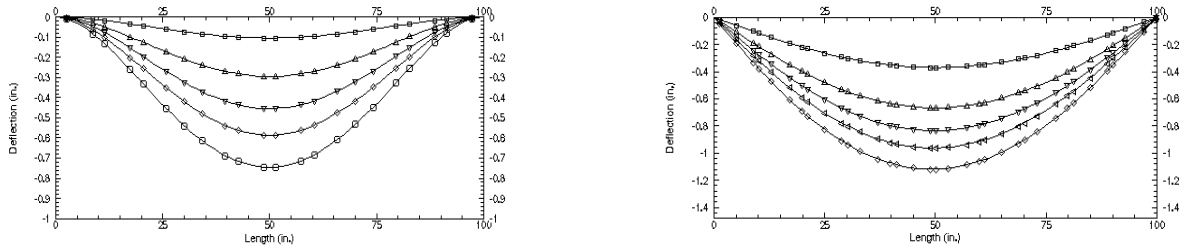

Fig. 3
Deformed shapes of the Timoshenko beam subject to different loadings for the clamped-clamped and pinned-pinned boundary conditions.

The mixed model, however, furnishes the axial force, shear force, and bending moment as a function of the length along the beam where as displacement model can furnish these results only as part of the post processing stage. Fig.1 presents the agreement between *hp*-spectral results of the Euler-Bernoulli beam theory with the series solutions. This figure also serves to validate the linear component of the EBT solutions. Fig.2 presents the deflections vs loads at the center of an EBT beam when subject to clamped-clamped and pinned-pinned boundary conditions with mixed formulations. As can be seen from the figure there is good agreement between the predictions of the center deflections from both models. Fig. 3 presents the deformed configurations of the TBT beam subject to clamped-clamped and pinned-pinned boundary conditions. The deformed configurations have been presented with a uniform loading subject to the beam at the following stages (to avoid clutter), q_0=[1 3 5 7 10] lb/in. It can be seen from the figure pinned-pinned beam deforms more as expected. Zero slope boundary condition at the ends of the clamped-clamped beam and zero deflections at the ends are evident. Fig. 4 presents the spectral convergence of the L^2 errors for the deflections and the slopes for the TBT beam model with series solutions. The spectral accuracy of the solutions with an increase in the p_{level} is evident from the figure. Fig. 5 presents the agreement between *hp*-SEM results for TBT with those obtained from the series solutions. The agreement between the results can be seen to be excellent. Fig. 6 presents load vs. deflection curves for the TBT model for both the clamped-clamped and pinned-

pinned boundary conditions for both the displacement based and mixed formulations. In Fig. 7 we present the shear force and bending moment at the end of TBT beam subject to clamped-clamped boundary conditions vs. the non-dimensional deflections when subject to increasing load steps for the beam dimensions mentioned in Table 9. An approximate parabolic variation of the shear and a linear variation of the moment is evident with increasing load parameters.

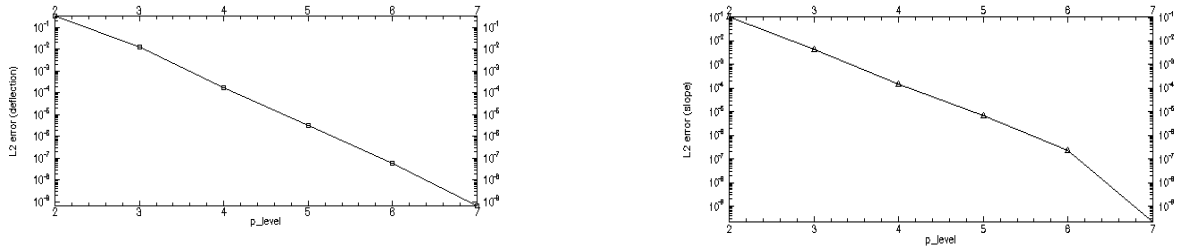

Fig. 4
Spectral convergence of the L_2 errors between the *hp*-SEM solutions and series solutions for TBT.

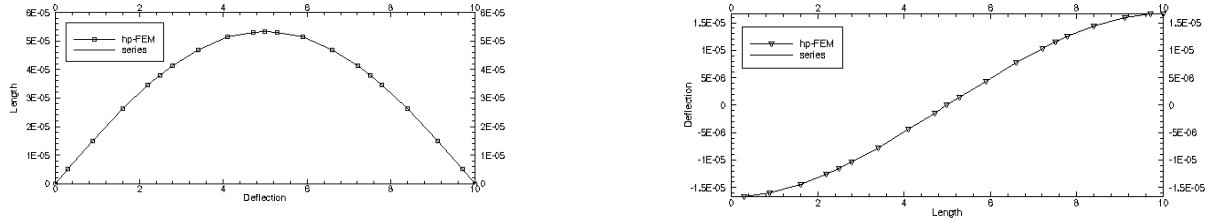

Fig. 5
Agreement between the hp-SEM results and series solutions for the TBT.

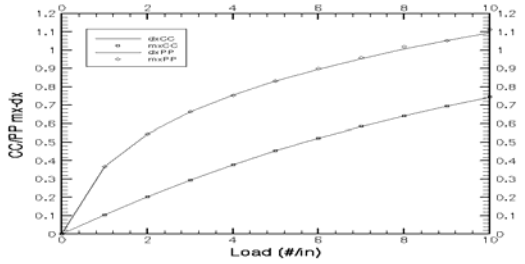

Fig. 6
Load vs. deflection curves CC/PP boundary conditions mixed/displacement based models for TBT.

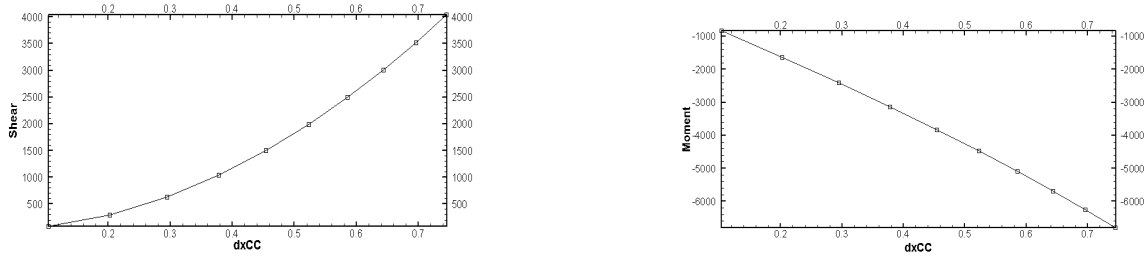

Fig. 7
Deflection vs. shear force and bending moment at the end of a clamped-clamped TBT beam.

13 CONCLUSIONS

Through this work we have demonstrated the usage of *hp*-SEM method as a viable tool for predicting the bending response of both Euler-Bernoulli beam and the Timoshenko beam models both for moderate to large deflections. We also advocate the usage of higher order spectral basis for predicting the bending response without the use of ad-hoc procedures of reduced and selective integration to obtain reliable results with *full-integration* techniques both for linear and non-linear problems. The maximum percentage error found between the selective and reduced integration results and the hp/spectral results was 1.56% which is lesser than the engineering accuracy of 2%. The usage of hp-SEM also alleviates the perennial problems of ill-conditioning of the stiffness matrices obtained with the usage of higher-order equi-spaced Lagrange basis.

REFERENCES

[1] Reddy J.N., 2004, *An Introduction to Non-Linear Finite Element Analysis*, Oxford University Press, NY.
[2] Severn R.T., 1970, Inclusion of shear deflection in the stiffness matrix for a beam element, *Journal of Strain Analysis* **5**: 239-241.
[3] Reddy J.N., Wang C.M., Lam K.Y., 1997, Unified Finite Elements based on the classical and shear deformation theories of beams and axisymmetric circular plates, *Communications in Numerical Methods in Engineering* **13**: 495-510.
[4] Reddy J.N., 1997, On Locking-free shear deformable beam finite elements, *Computer Methods in Applied Mechanics and Engineering* **149**: 113-132.
[5] Arciniega R.A., Reddy J.N., 2007, Large deformation analysis of functionally graded shells, *International Journal of Solids and Structures* **44**: 2036-2052.
[6] Karniadakis G.K., Sherwin, S., 2004, *Spectral/hp Element Methods for Computational Fluid Dynamics,* Oxford Science Publications, London.
[7] Bar-Yoseph P.Z., Fisher D., Gottlieb O., 1996, Spectral element methods for nonlinear spatio-temporal dynamics of Euler-Bernoulli beam, *Computational Mechanics* **19**: 136-151.
[8] Melenk J.M., 2002, On Condition numbers in *hp*-FEM with Gauss-Lobatto-based shape functions, *Journal of Computational and Applied Mathematics* **139**: 21-48.
[9] Maitre J.F., Pourquier O., 1996, Condition number and diagonal preconditioning: comparison of the p-version and the spectral element methods, *Numerische Mathematik* **74**: 69-84.
[10] Cook R.D., Malkus D.S., Plesha M.E., Witt R.J., 2002, *Concepts and Applications of Finite Element Analysis,* John Wiley and Sons Inc., NY.
[11] Edem I.B. 2006, The exact two-node Timoshenko beam finite element using analytical bending and shear rotation interdependent shape functions, *International Journal for Computer Methods in Engineering Science and Mechanics* **7**: 425-431.
[12] Pontaza J.P., Reddy J.N., 2004, Mixed Plate Bending elements based on Least Squares Formulations, *International Journal for Numerical Methods in Engineering* **60**: 891-922.
[13] Reddy J.N., 2002, *An Introduction to Finite Element Method*, Mc.Graw Hill, NY.
[14] Osilenker B., 1999, *Fourier Series in Orthogonal Polynomials,* World Scientific.
[15] Prabhakar V., Reddy J.N., 2007, Orthogonality of Modal basis in *hp* finite element models, *International Journal for Numerical Methods in Fluids* **54**: 1291-1312.
[16] Reddy J.N., 2007, Non local theories for bending, buckling, and vibration of beams, *International Journal of Engineering Science* **45**: 288-307.
[17] Reddy J.N., 1999, *Theory and Analysis of Elastic Plates*, Taylor and Francis, London.